

SOURCE
End of Summer Paper
Comparative Study of Corrosion Behavior in Additively
Manufactured and Wrought Stainless Steel
Author:
Zhansar Zhaparov, B.S. Mechanical Engineering
Mentors:
Dr. Zechariah Pfaffenberger, Department of Physics
Prof. Lydia Kisley, Department of Physics and Chemistry

Introduction

Corrosion, a chemical deterioration or destruction of a material, is a multi-billion-dollar industry problem that directly impacts the safety of our daily lives. It affects critical systems such as bridges, vehicles, planes, water supply networks, and medical implants. The issue is especially pressing in the aggressive marine environments, where highly acidic and chloride-rich substances can alter the chemical properties and mechanical behavior of the materials and structures (1). If left unchecked, corrosion can lead to severe health consequences and serious monetary losses. It was estimated that the total direct cost of corrosion in the US is over \$276 billion annually, equivalent to 3.1 percent of the US GDP (2).

Despite being a major problem, corrosion behaviour is not fully understood and documented, while existing research mainly focuses on invasive and weak-magnification techniques. Different electrochemical methods including open circuit potential, linear polarization resistance, impedance spectroscopy, and cyclic polarization are all widely used ways to quantify corrosion rates, but they frequently disturb passive films formed on the surface and initiate pitting corrosion (3). Techniques such as Scanning electron microscopy (SEM), scanning tunneling microscopy (STM), and atomic force microscopy (AFM) could be effective to analyze both the spatial and rate information on corrosion initiation at nano- and microscale levels, but these methods are ex-situ, showing the before-after relationships only of samples removed from the corrosive environment (4). In some cases, materials also need to be immersed in a solution for months or years to obtain accurate and representative corrosion rate measurements (5).

Fluorescence microscopy offers both non-invasive and in situ analysis, and is capable of probing materials down to the single-molecule scale. Fluorescence itself is a form of luminescence in which a material absorbs light at one wavelength and re-emits it at a longer wavelength. Specifically, the process initiates when a chemical called a fluorophore absorbs a blue photon, exciting its electrons to a higher energy state. In the vibrational relaxation process, the fluorophore electrons return to their ground state, releasing the remaining energy as light. A highly sensitive camera then detects this red-shifted fluorescence emission. In corrosion studies, molecules that are initially non-fluorescent can undergo chemical transformations interacting

with corrosion products, such as metal ions or electrons, thus becoming fluorescent and emitting detectable light (Figures 1 and 2).

This study focuses on the comparison of wrought and additively manufactured stainless steel, focusing on the impact of microstructural differences on corrosion resistance. The relation between the elemental composition and corrosion resistance will be investigated utilizing single-molecule fluorescence and scanning electrochemical microscopy (SEM). The bottom-up approach to understanding localized corrosion pits both qualitatively and quantitatively will be developed. The study will also contribute to the broader and deeper understanding of additive manufacturing processes and find the optimal printing parameters specific to the printer's technology.

Background

Additively manufactured metals offer a promising domain for reducing production costs and improving the quality of the final product. Unlike the traditional subtracting machining, the 3D printing technique leaves minimal waste and allows faster prototyping and iteration. It is a powerful technique that introduces complex shapes in large-scale manufacturing, eliminating design and flexibility constraints of conventional manufacturing. It also often outperforms conventional steels at yield strength and tensile ductility characteristics (6). It was estimated that the production cost savings from additive manufacturing adoption range from 36 to 46% (7). Moreover, the additional indirect savings value from operating costs would even be greater than the manufacturing cost advantage (8). However, 3D printing has its own limitations including restricted build size, lower structural integrity, and complicated post processing. The various mechanical and material properties, such as corrosion resistance, will heavily depend on the print settings and can differ remarkably from their wrought counterparts (9).

The opinions on the corrosion resistance of 3D-printed metals compared to traditional counterparts differ a lot across the literature. To narrow the scope of this research, the paper will look into two commonly used stainless steels in the industry. Specifically, austenitic SS304L and SS316L are both corrosion resistant steels that are widely used in medical, pharmaceutical, food and beverage, chemical processing, and industrial fields. Their relatively low cost, versatile application, and great mechanical properties have been a significant advantage over other SS grades. The presence of chromium greatly improves their corrosion-resistant properties because of a protective film that forms on a metal surface in response to the oxidizing environment.

The main corrosion types affecting both alloys are uniform corrosion, pitting corrosion, crevice, and stress corrosion cracking. Researchers highlight that pitting corrosion is a major issue for additively-manufactured SS (10). Some researchers indicate that higher defects concentration such as lack-of-fusion, gas pores, cracks, and keyholes on the 3D-printed metals surface significantly decrease their corrosion resistance (11). Metal 3D printing inherently involves layer-by-layer rapid heating and cooling, which creates steep thermal gradients that induce the tensile and compressive stresses within the 3D-printed material (12). These stresses potentially cause morphological deformities and microcracks on the metal's surface. 3D-printed

steels might also have higher corrosion susceptibility because of the rougher surface finish and larger average grain size, creating more contact area and additional space for chemical attack (13, 14). However, a smoother surface is not necessarily optimal for the most corrosion resistance, since ideal roughness value depends on intended application and cost-benefit analysis (9). Moreover, unlike conventional steel, 3D-printed steel is expected to exhibit a heterogeneous composition due to its powder-based manufacturing process, which might otherwise improve corrosion resistance (6). On the other hand, the inhomogeneity in grain size and small grain aggregations formed in the laser deposition process can facilitate pitting corrosion (14). 3D-printed SS316L also has molybdenum segregation at the sub-grain boundaries due to heavy atoms unable to complete diffusion in a rapid cooling rate (10). This separation causes microgalvanic corrosion between sub-grains and sub-grain boundaries and reduces the self-repairing ability of a chromium protective film, making AM SS316L more susceptible to the pitting corrosion. Conversely, another study showed that AM SS316L was less susceptible to the pitting corrosion, but the stress relieving heat post-treatment mechanism was applied to the sample. The overall lower stability of a passive layer and higher corrosion susceptibility are also true for the wrought SS304L (14). However, the protective film of AM SS316L is around 1.7 times thicker and more compact than of conventional SS316L due to higher dislocation density and sub-grain boundaries, indicating better passivation kinetics and film adherence. Still, the 3D-printed versions of SS304L and SS316L both show worse general corrosion resistance measured by chronopotentiometry (CP), open circuit potential (OCP), and cyclic potentiodynamic polarization (CPP) tests (10). The main difference between both alloys is the containment of 2-3% molybdenum in SS316L to chemical composition of SS304L, which is deemed to improve the corrosion resistance performance in chloride-containing and highly acidic environments (16). It is important to recognize that different printing methods cause different structural factors, including surface roughness, residual stresses, oxide inclusions, build orientation, and post-processing conditions affect the results, causing discrepancies in the authors' conclusions.

Methodology

As one of the most widely used materials in the industry and research, which also has powder analogs for additive manufacturing purposes, stainless steels 304L and 316L from McMaster-Carr were studied in the corrosion process. Both 304L and 316L grades are modified 304 and 316 versions with a lower carbon content of around 0.03% or less (0–2.0 Mn, 0.0 –1.0 Si, 0.0 –0.11 Ni, 0.0 –0.5 P, 0.0 –0.03 S, 8.0–15.0 Ni, 17.5 –19.5 Cr, Fe balance wt%). However, 316L has 2-3% molybdenum to the 304 composition, deemed to stabilize the protective chromium film and show better corrosion resistance in chloride-containing environments.

For additive manufacturing purposes, the Aconity MIDI 3D printer in Professor Laura Bruckman's lab in the Department of Materials Science and Engineering was used to fabricate metal samples from powder analogs of SS304L and SS316L with the same composition. The Aconity MIDI operates on laser powder bed fusion (LPBF) technology, known for its high

precision and excellent surface finish. Since the lab was only recently introduced to the printer, they tried various settings for their prints. SS316L samples were printed with 175 Watts power, 900 millimeters per second scan speed, 30 micrometers layer height, and 80 micrometers hatch spacing following an island pattern without contour. These parameters were later adjusted for SS304L to increase the quality of the prints according to the manufacturer's recommended settings: 150 Watts power, 900 mm/s scanning speed, 30 micrometers layer height, and 80 micrometers hatch spacing following an island pattern with contour. The sample sizes were selected to replicate the traditional stainless steel cubes that were cut on the horizontal bandsaw in Think[box].

Both traditional and 3D-printed samples were put in an epoxy cure to expose only the cross-sectional side of the sample to the environment for more consistent results. They were later polished on the exposed sample surfaces with 60, 400, 600, 800, and 1200 grits of SiC sandpaper. The samples were cleaned by ethanol ultrasonication and dried with nitrogen before the experiment. When not undergoing active data collection, the samples were stored in a portable desiccator vacuum chamber. Before the sample immersion, a scanning electron microscope with an energy dispersive X-ray spectroscopy tool (SEM-EDS) scanned and analyzed the sample surfaces and their elemental composition for any possible defects or contamination. A ThermoFisher Apreo 2S machine at Swagelock was used for SEM-EDS analysis. The images were taken at 500x, 6500x, and 20000x magnifications, and SEM analysis was conducted at 5000x magnification. The beam parameters were set to 5.00 kilovolts, 50 picoamperes, and 10 millimeters working distance for SEM, and 0.8 nanoamperes and 20.0 kilovolts for EDS.

After imaging, both traditional and 3D-printed samples were immersed in separate 10 milliliter aqueous solutions of 5 micromolar resazurin and PGSK dyes with 3.5 wt% NaCl in 20 millimolar HEPES buffer, pH = 7.4 each. The samples were then placed in an IncuShaker at room temperature and a shaking speed of 50 revolutions per minute. Small amounts of solution (250 microliters) were taken out from each sample for the time intervals of 0, 0.5, 1, 1.5, 2, 3, 4, 5, 6, 8, 12, 24, 32 hours and stored in the fridge (0-5°C). Later, each sample was diluted with a 20 mM HEPES buffer to 2.0 milliliters and analyzed using the Jasco FP-8350 fluorimeter. The fluorescence measurements were taken on both dyes at a 500 Volts beam power supply, 2.5 nanometers excitation and emission bandwidth, 0.1 seconds response time, 0.5 nanometers data interval with a 500 nanometers per minute scan speed. The PGSK dye was removed after a second experiment and is not documented in the results of this paper, as we did not see a clear turn-off response. On the other hand, resazurin was working well at 488 nanometers excitation wavelength and 500 - 650 nanometers emission spectra, detecting the anodic corrosion reaction $\text{Fe(s)} \rightarrow \text{Fe}^{2+} + 2\text{e}^-$.

After the sample tests, the Apreo 2S capabilities were used again to examine the morphology of the final corroded part, analyzing changes in porosity, grain structure, and surface roughness.

Findings and Results

upon

After conducting and collecting data from three experiments, I constructed a graph of intensity vs. time to compare the corrosion rates of both 3D-printed and conventional SS316L at an excitation wavelength of 561 nanometers (Figure 3). Despite the 3D-printed cube sample showing consistently higher intensity at each time point, the intersecting error bars do not provide sufficient evidence of the difference between traditional and 3D-printed SS316L corrosion rates. SS316L stays at approximately the same intensity level, most likely due to a compact film formation that prevents general and pitting corrosion. However, the increase in intensity can be attributed to the anodic corrosion process.

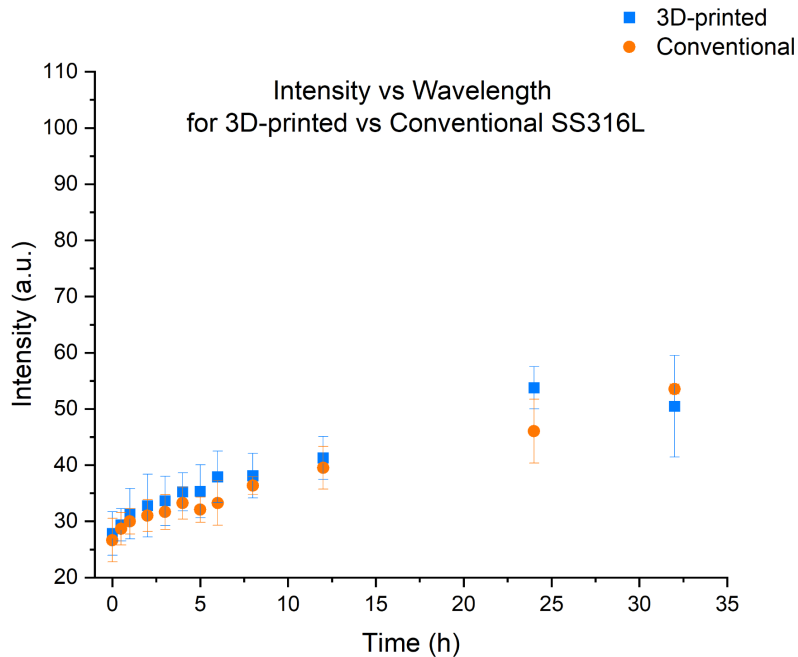


Figure 3. Dotplot of Intensity vs Time with the error bars as standard deviations with n = 3

Similar data for three experiments was collected for SS304L, constructing an intensity vs time graph at 561 nanometers (Figure 4). Both graphs start at around the same 25-30 intensity range, but the corrosion rate of SS304L is significantly higher than that of SS316L, as indicated by a drastic intensity change starting from 6 hours. A more noticeable gap between traditional and AM SS304L corrosion rates is observed, where the 3D-printed material corrodes seemingly less overall. However, the intersecting error bars again do not provide enough evidence of the difference between traditional and 3D-printed SS304L corrosion rates.

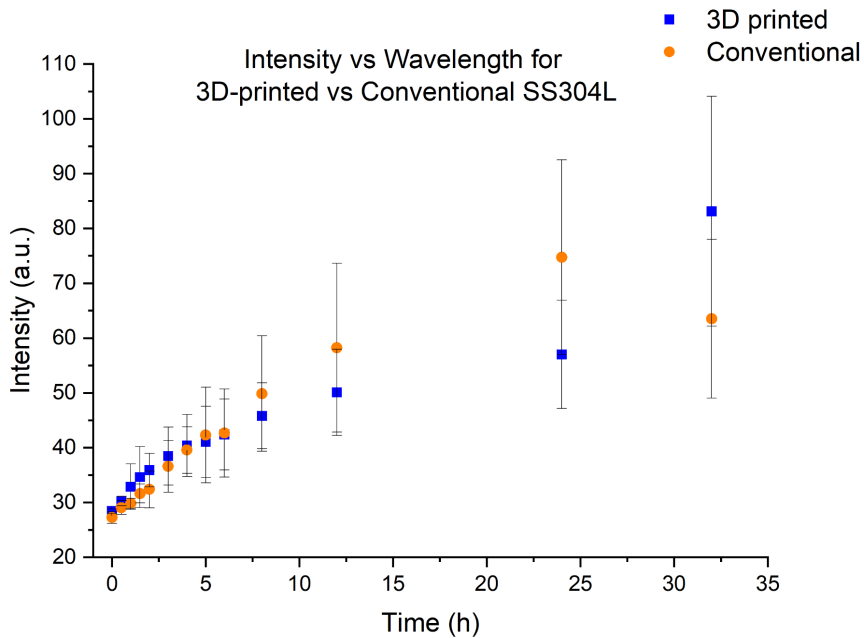


Figure 4. Dotplot of Intensity vs Time with the error bars as standard deviations with $n = 3$

Figures 5 and 6 display the same data from above in an exponential logarithmic form. It can be inferred that the corrosion rates of SS304L and SS316L do not follow an exponential trend. The real corrosion rate can be quantified based on the slope data in Figure 7. Figures 8 and 9 are dotplots of Resorufin concentration vs time, where concentrations are correlated to intensity changes from the initial solution intensity at time = 0 hours. Thus, the molar rates can be calculated, knowing the linear-fit slope from these graphs and volume (V) of the solution, according to Equation 1.

$$r_{Res} \text{ [mol/s]} = V \cdot \frac{dC_{Res}}{dt} \quad (1)$$

Considering that resazurin to resorufin reduction is a 2-electron process, we can calculate the electron rate according to Equation 2. F is a faraday's constant and v is electron quantity.

$$I \text{ [A]} = F \cdot \dot{n}_{e^-} = F \cdot \nu \cdot r_{Res} \quad (2)$$

The current density can be derived through the calculated currency and the known exposed surface area (Equation 3)

$$i \text{ [A/cm}^2\text{]} = \frac{I}{A} \quad (3)$$

upon

Faraday's law of electrolysis relates the mass of a substance produced to the electrical current that has been put through the electrolyte over time. Equation 4 can be transformed into Equation 5 by converting the mass into volume times density and dividing the whole equation by area to obtain corrosion rate.

$$m = \frac{I \cdot t \cdot EW}{F} \quad (4)$$

$$\text{Corrosion rate} = \frac{i \cdot EW}{F \cdot \rho} \quad (5)$$

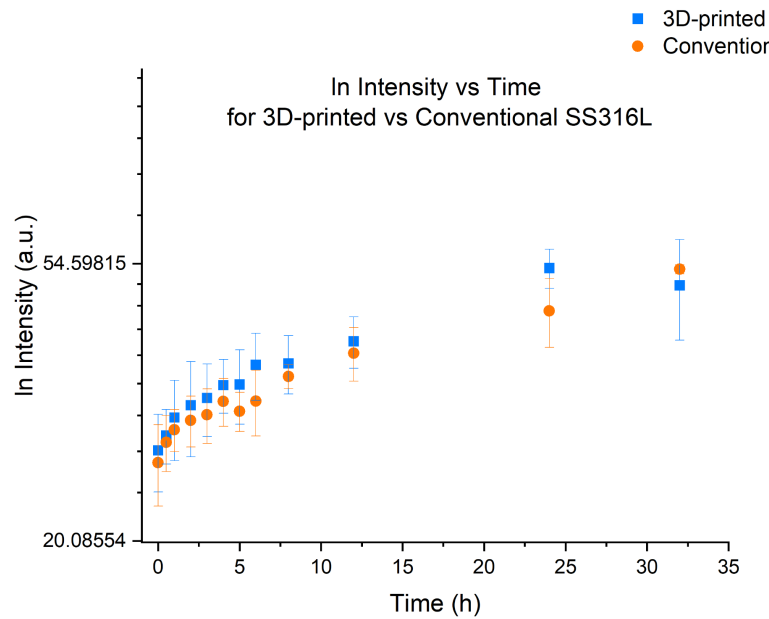


Figure 5. Exponential logarithm of Intensity vs Time for SS304L

upon

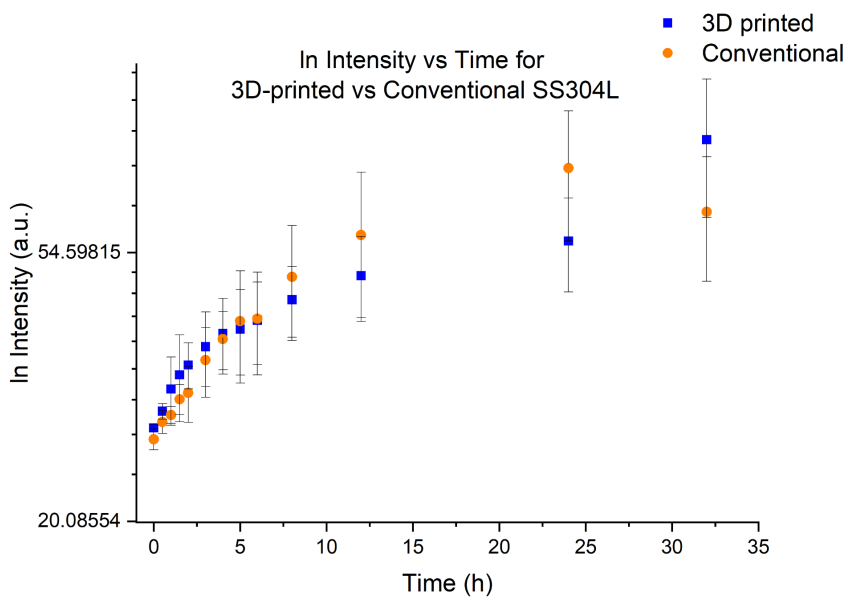


Figure 6. Exponential logarithm of Intensity vs Time for SS304L

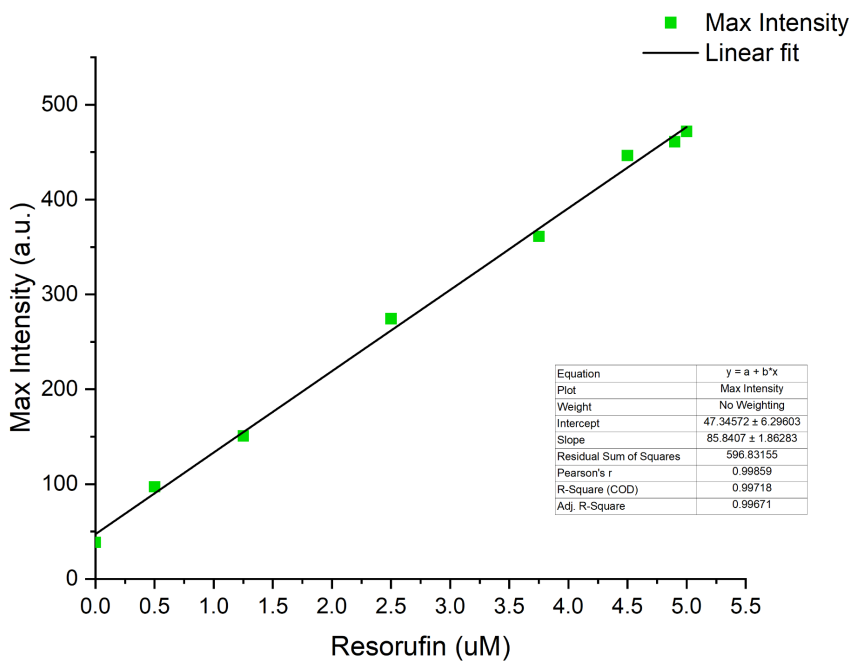


Figure 7. Intensity vs Resorufin concentration linear-fit graph

upon

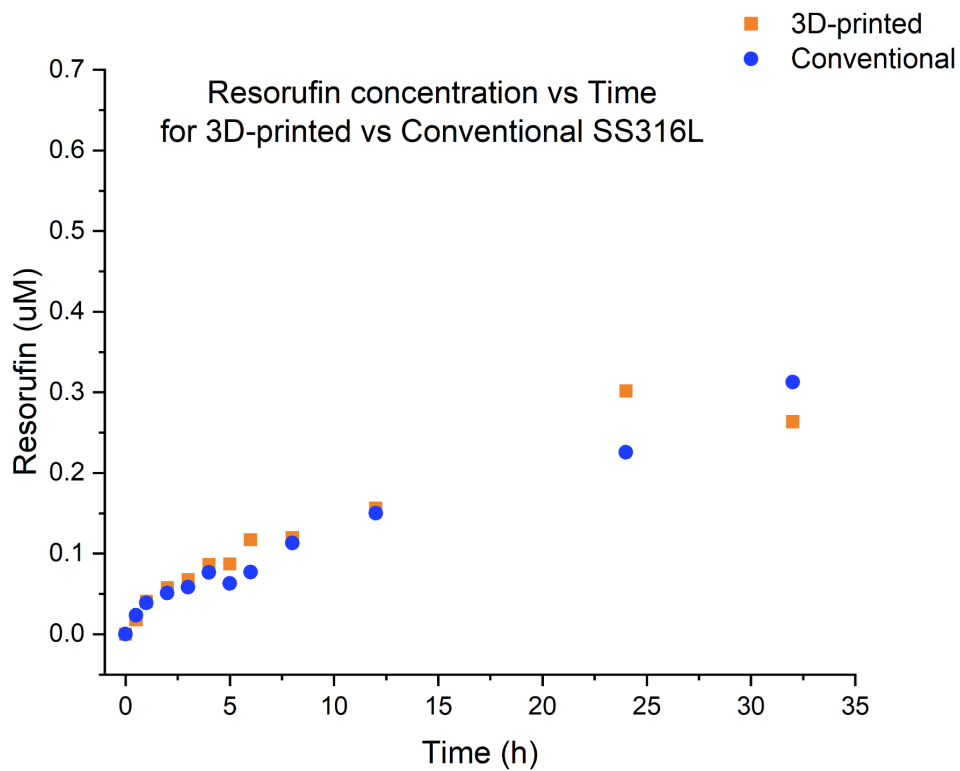


Figure 8. Resorufin concentration vs Time for SS316L

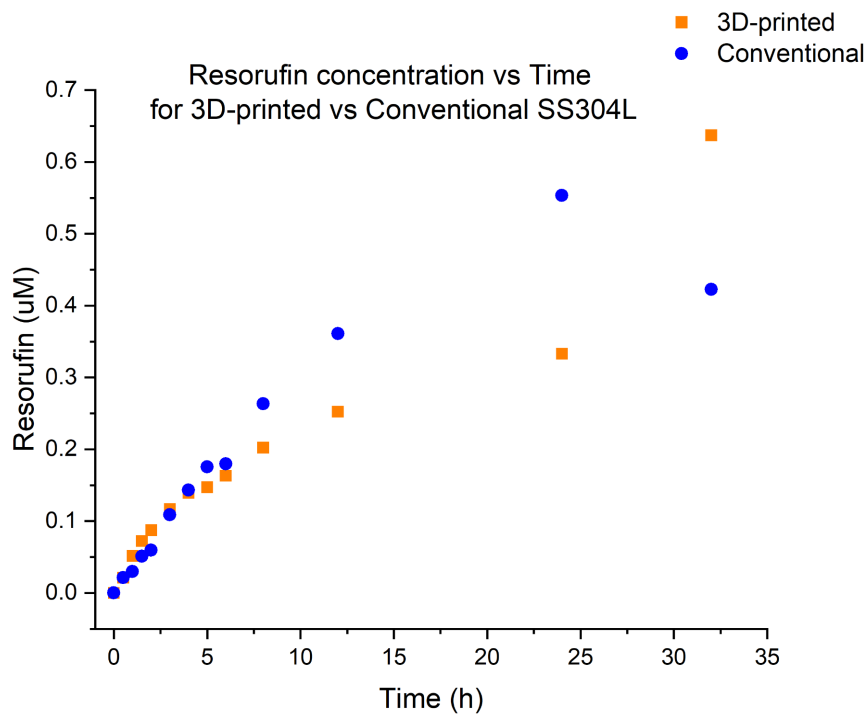


Figure 9. Resorufin concentration vs Time for SS304L

upon

The estimated corrosion rates are displayed in Table 1. A consistent decrease in corrosion rate with increasing time can be observed across all samples. 3D-printed SS304L corrodes approximately the fastest in the first hour, but ends up the slowest at 24 hours. Traditional SS304L, on the other hand, corrodes the fastest at 0.192 millimeters per year in later times. Traditional SS316L corrodes more slowly than both 3D-printed SS316L and traditional SS304L across all time points. Overall, both 3D-printed and traditional SS316L corrode more slowly than SS304L.

		Time (h)	1	6	24
SS316L	3D-printed	Molar Rate (mol/s)	4.595E-10	3.021E-10	1.213E-10
		Current (A)	8.867E-05	5.830E-05	2.341E-05
		Current density (A/mm ²)	5.541E-07	3.643E-07	1.463E-07
		Corrosion Rate (mm/year)	5.50E-01	3.62E-01	1.45E-01
	Traditional	Molar Rate (mol/s)	3.06E-10	1.39E-10	6.30E-11
		Current (A)	5.90E-05	2.69E-05	1.22E-05
		Current density (A/mm ²)	3.69E-07	1.68E-07	7.60E-08
		Corrosion Rate (mm/year)	3.66E-01	1.67E-01	7.54E-02
SS304L	3D-printed	Molar Rate (mol/s)	6.104E-10	6.775E-10	6.710E-11
		Current (A)	1.178E-04	1.307E-04	1.295E-05
		Current density (A/mm ²)	7.361E-07	8.170E-07	8.092E-08
		Corrosion Rate (mm/year)	7.31E-01	8.11E-01	8.03E-02
	Traditional	Molar Rate (mol/s)	1.77E-10	4.40E-11	1.60E-10
		Current (A)	3.42E-05	8.49E-06	3.09E-05
		Current density (A/mm ²)	2.14E-07	5.31E-08	1.93E-07
		Corrosion Rate (mm/year)	2.12E-01	5.27E-02	1.92E-01

Table 1. Estimated corrosion rate variables for SS304L and SS316L based on the Resorufin vs Time graph linear-fit slope equation

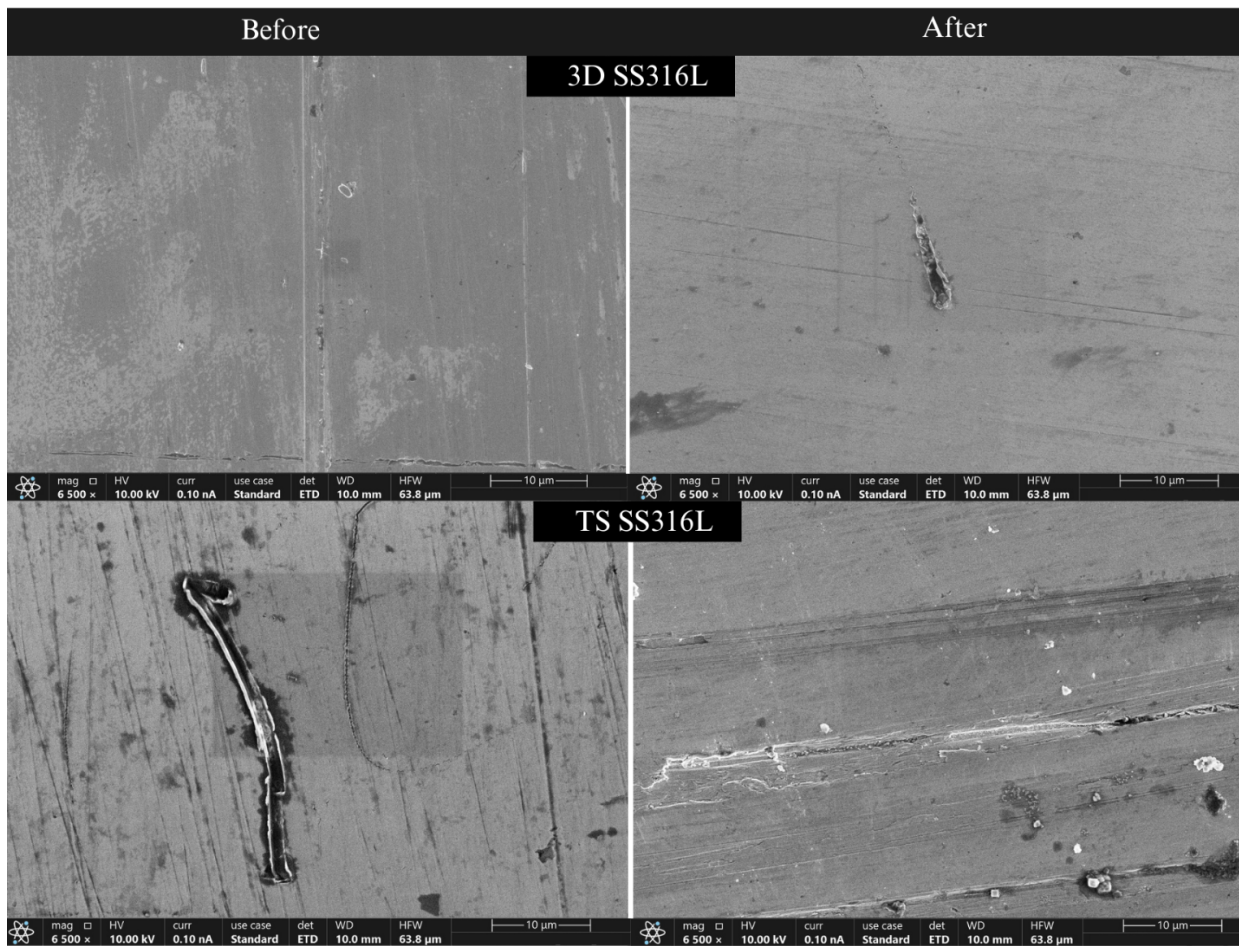
The comparison between 3D-printed and traditional steel is shown in Figures 10 and 11. The current SEM-EDS analysis was limited in the available time, so only the picture of one specific area was taken at each magnification. The images shown in Figure 10 were captured in 6500x.

The striation lines, seen on all presented surfaces, are the result of the 1200-grit surface polish. Evident black spots on the surfaces, which might be confused for pits, are carbon particles shown in the EDS section (Figures 12-15). Because the presence of carbon in SS316L and SS304L is very low (<0.03%), the large carbon particles are most likely surface contaminants. Some additional precipitates can be observed on the traditional SS316L and SS304L.

upon

The 3D-printed surface looks smoother overall for both SS316L and SS304L, but still has some minor defects. Traditional SS316L also has some noticeable defects before and after corrosion. Different grooves a few micrometers long can be seen in the corrosion images of traditional SS316L. Some deformities or cracks can be noticed on the right side of the 3D-printed SS304L surface after immersion. Some additional black spots can also be observed on the traditional SS304L, which might correspond to possible localized pits.

Further analysis is required to establish pitting corrosion using single-fluorescence microscopy and electrochemistry methods, as the current SEM-EDS method provides only visual data across the large surface area.



upon

Figure 10. Before vs After Immersion SEM Images of SS316L at 6500x magnification

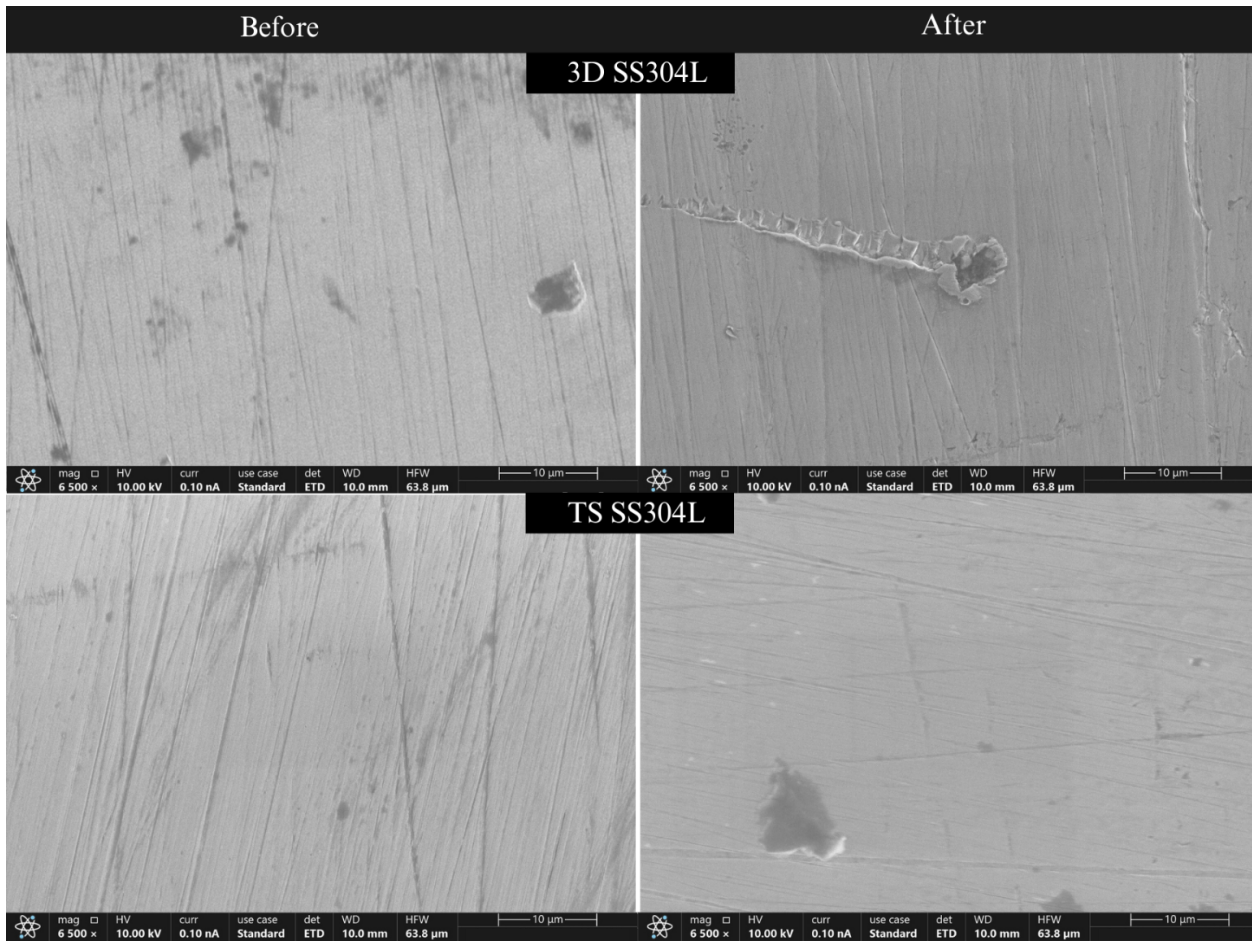


Figure 11. Before vs After Immersion SEM Images of SS304L at 6500x magnification

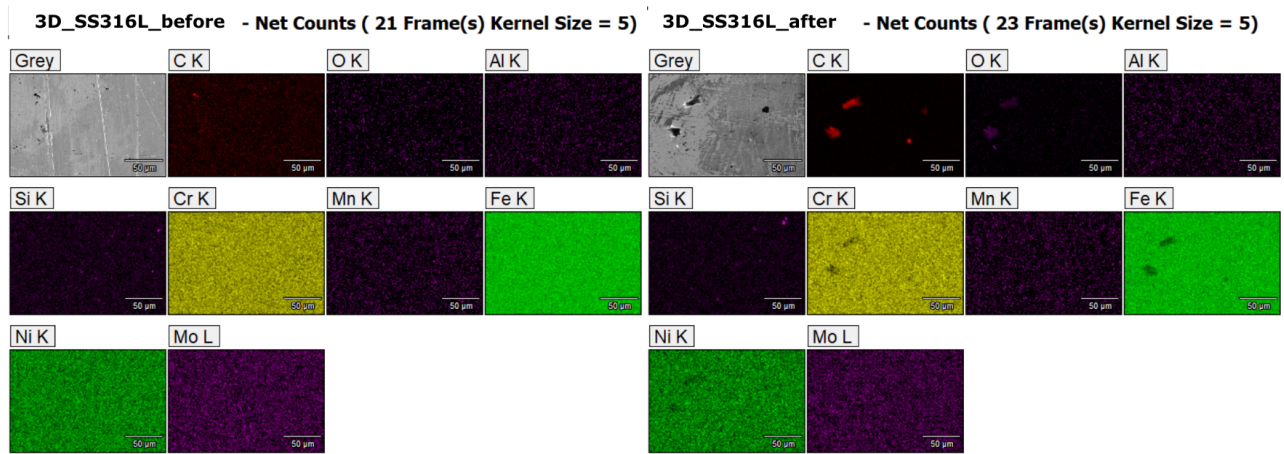


Figure 12. Before vs After Immersion EDS images of 3D-printed SS316L at 2000x magnification

upon

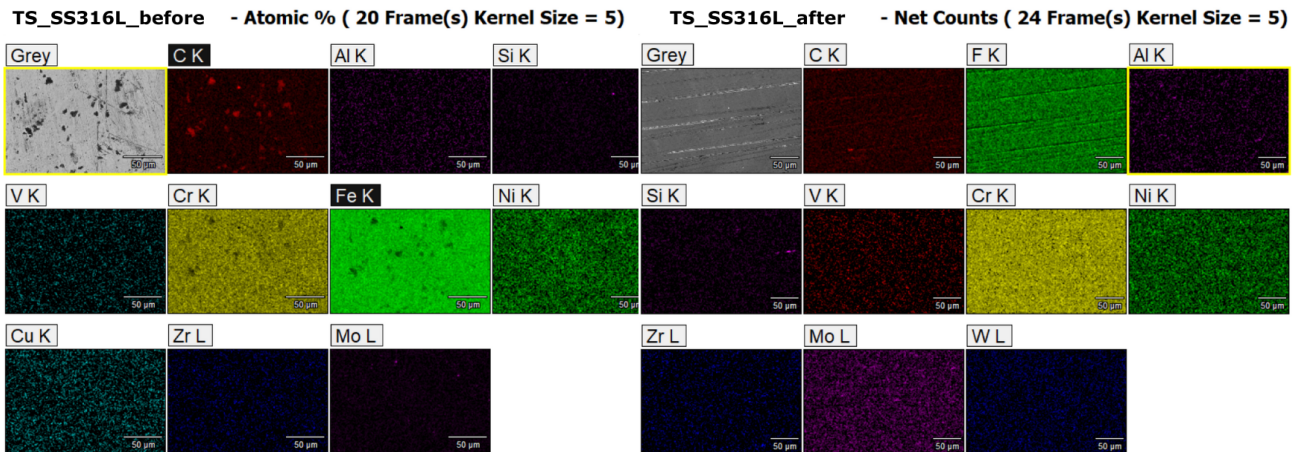


Figure 13. Before vs After Immersion EDS images of traditional SS316L at 2000x magnification

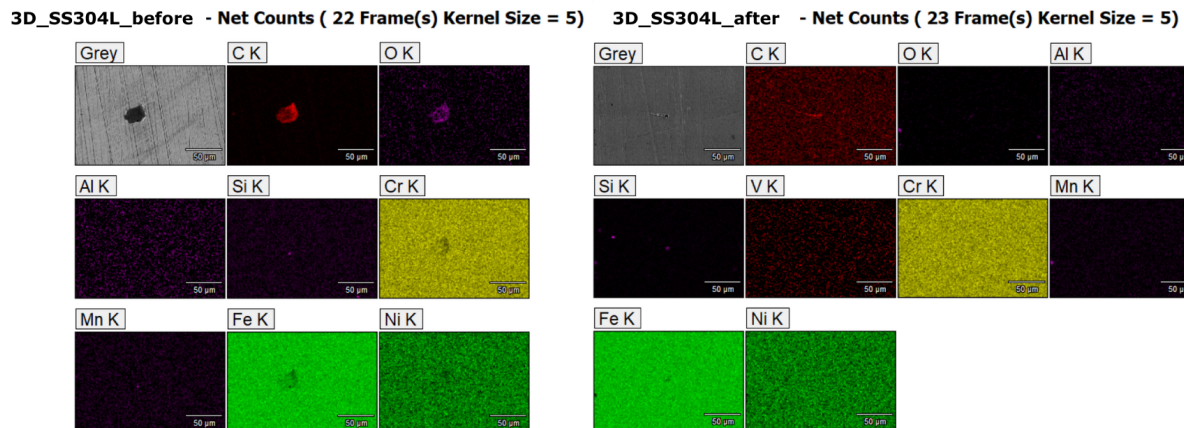
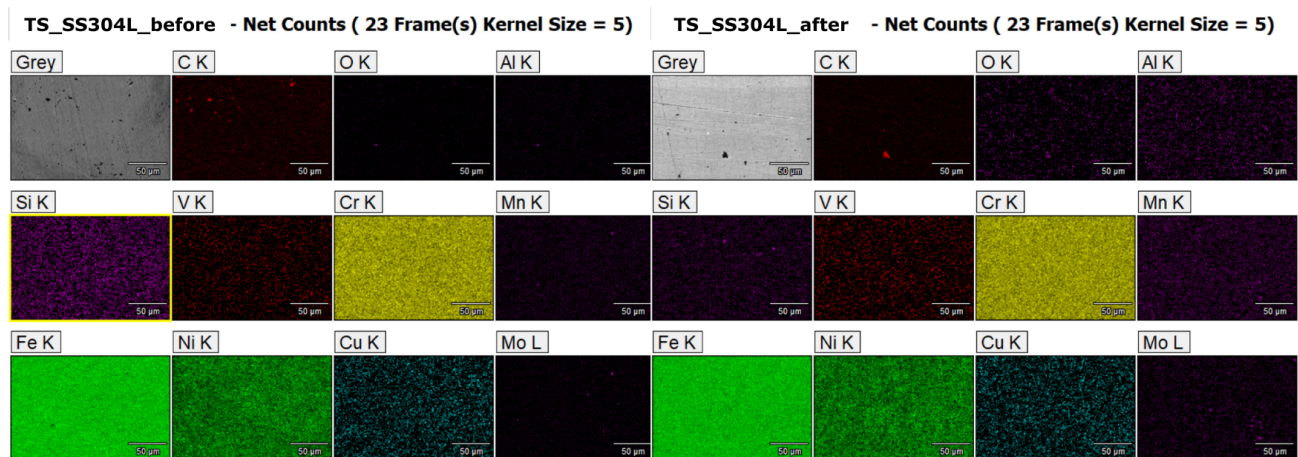


Figure 14. Before vs After Immersion EDS images of 3D-printed SS304L at 2000x magnification



upon

Figure 15. Before vs After Immersion EDS images of traditional SS304L at 2000x magnification

Conclusion

This study investigated the corrosion resistance differences between additively manufactured and conventionally manufactured stainless steel. It used fluorescence microscopy to derive the corrosion rates of both SS316L and SS304L. The bulk fluorescence measurements did not prove any substantial difference between additively manufactured and wrought stainless steel. However, it was shown that the corrosion rate of SS316L is generally slower than that of SS304L, consistent with the literature described in this paper. Moreover, the 3D-printed SS316L exhibited a slower corrosion rate than its wrought counterpart, whereas the opposite was true for SS304L. These results can be attributed to the surface morphology, where it was generally observed that traditional SS316L had more surface precipitates and potential cracks than 3D-printed SS316L, which was opposite for SS304L. However, deeper analysis with correlative imaging, where single-molecule microscopy will map the in situ locations of corrosion reactions, and SEM combined with energy-dispersive spectroscopy (SEM-EDS) will provide ex situ grain boundary and elemental images, is needed.

Acknowledgement

I want to thank my mentor, Dr. Zechariah Pfaffenberger, and principal investigator, Dr. Lydia Kisley, for providing me with extensive support and resources that were essential to the completion of this study. I would also like to thank the Undergraduate Research Office and Case Alumni Foundation for providing me with the necessary summer research funding.

References

1. Dhaiveegan, P., et al. “Corrosion Behavior of 316L and 304 Stainless Steels Exposed to Industrial-Marine-Urban Environment: Field Study.” *RSC Advances*, vol. 6, no. 53, 2016, pp. 47314–47324, <https://doi.org/10.1039/c6ra04015b>
2. Koch, G. H., Brongers, M. P. H., Thompson, N. G., Virmani, Y. P., & Payer, J. H. (2005). Cost of corrosion in the United States. *Handbook of Environmental Degradation of Materials*, 3–24. <https://doi.org/10.1016/b978-081551500-5.50003-3>
3. D. Delgado López, Schreiner, W. H., S.R. de Sánchez, & Silvia Noemi Simison. (2003). The influence of carbon steel microstructure on corrosion layers. *Applied Surface Science*, 207(1-4), 69–85. [https://doi.org/10.1016/s0169-4332\(02\)01218-7](https://doi.org/10.1016/s0169-4332(02)01218-7)
4. Saini, A., Messenger, H., & Kisley, L. (2020). Fluorophores “Turned-On” by Corrosion Reactions Can Be Detected at the Single-Molecule Level. *ACS Applied Materials & Interfaces*, 13(1), 2000–2006. <https://doi.org/10.1021/acsami.0c18994>
5. Ron, T., Levy, G. K., Dolev, O., Leon, A., Shirizly, A., & Aghion, E. (2019). Environmental Behavior of Low Carbon Steel Produced by a Wire Arc Additive Manufacturing Process. *Metals*, 9(8), 888. <https://doi.org/10.3390/met9080888>
6. Wang, Y. Morris, et al. “Additively Manufactured Hierarchical Stainless Steels with High Strength and Ductility.” *Nature Materials*, vol. 17, no. 1, 30 Oct. 2017, pp. 63–71,

upon

- www.nature.com/articles/nmat5021, <https://doi.org/10.1038/nmat5021>.
7. Baumers, Martin, et al. "Informing Additive Manufacturing Technology Adoption: Total Cost and the Impact of Capacity Utilisation." *International Journal of Production Research*, vol. 55, no. 23, 6 June 2017, pp. 6957–6970, <https://doi.org/10.1080/00207543.2017.1334978>. Accessed 29 Mar. 2020.
 8. GE Aerospace. "Manufacturing Milestone: 30,000 Additive Fuel Nozzles | GE Aerospace News." www.ge aerospace.com, 4 Oct. 2018,
www.ge aerospace.com/news/articles/manufacturing/manufacturing-milestone-30000-additive-fuel-nozzles.
 9. Verma, Chandrabhan, et al. "Review on Corrosion-Related Aspects of Metallic Alloys Manufactured with Laser Powder Bed-Fusion (LPBF) Technology." *Progress in Additive Manufacturing*, 28 Sept. 2024, <https://doi.org/10.1007/s40964-024-00810-x>. Accessed 9 Mar. 2025.
 10. Nie, Jingjing, et al. "Corrosion Mechanism of Additively Manufactured 316 L Stainless Steel in 3.5 Wt.% NaCl Solution." *Materials Today Communications*, vol. 26, 1 Mar. 2021, p. 101648, www.sciencedirect.com/science/article/pii/S2352492820326593,
<https://doi.org/10.1016/j.mtcomm.2020.101648>.
 11. Du, C., Zhao, Y., Jiang, J., Wang, Q., Wang, H., Li, N., & Sun, J. (2023). Pore defects in Laser Powder Bed Fusion: Formation mechanism, control method, and perspectives. *Journal of Alloys and Compounds*, 944, 169215. <https://doi.org/10.1016/j.jallcom.2023.169215>
 12. Fang, Ze-Chen, et al. "Review on Residual Stress in Selective Laser Melting Additive Manufacturing of Alloy Parts." *Optics & Laser Technology*, vol. 129, Sept. 2020, p. 106283, <https://doi.org/10.1016/j.optlastec.2020.106283>.
 13. Toloei, A. S., et al. "Simultaneous Effect of Surface Roughness and Passivity on Corrosion Resistance of Metals." *Materials Characterisation VII*, 22 Apr. 2015, www.witpress.com/Secure/elibrary/papers/MC15/MC15032FU1.pdf,
<https://doi.org/10.2495/mc150321> Accessed 7 Apr. 2023.
 14. Saberi, Leila, et al. "Corrosion of Additively Manufactured Stainless Steel 304L in Relation to Grain Texture and Process-Induced Defects: A Localized Analysis." *Materials Characterization*, 1 Dec. 2024, pp. 114692–114692,
<https://doi.org/10.1016/j.matchar.2024.114692>. Accessed 19 Aug. 2025.
 15. Sakthivel N (2018) Analysis of wear and corrosion properties of 316 L stainless steel additively manufactured using laser engineered net shaping (Lens®). Oklahoma State University, Oklahoma
 16. Lillard, R. S. "A Review of Corrosion Issues Related to Uranyl Nitrate Base Aqueous Homogeneous Reactors." *Corrosion Engineering, Science and Technology*, vol. 45, no. 3, June 2010, pp. 194–203, <https://doi.org/10.1179/147842210x12659647007121>. Accessed 12 Mar. 2025.

upon

II. Reflection about the research experience and future plans

Please pause and reflect about the research experience. In doing so, you may want to consider any of the following:

- What did you learn from the experience?

Over the summer, I was exposed to a wide range of experiences, gaining deeper insight into academia and the research environment. I learned a great deal about conducting wet lab experiments, received training on the SEM-EDS microscope, and became proficient in using Origin analysis software. I also gave presentations within my research group, learning how to speak and present in an academic environment. Moreover, I read a lot of scientific literature, sharpening my critical thinking skills.

- How were your summer project plans different from your application proposal? What happened during the research process that changed your project direction?

At the beginning of the summer, I tried my best to develop a more specific research plan than the one I described in my application. It helped me to structure my work, but also look at it more realistically. I had to abandon the idea of doing single-molecule microscope analysis because I had an issue with choosing responsive fluorescent dyes for my initial corrosion rate experiments. I also had delays in my work that did not depend on me, since I had to work with another lab and the Swagelok Center of Surface Analysis. Their equipment broke multiple times, so I had to reschedule my training and some experiments.

- Was this summer research experience positive (or not)? How did this summer research experience meet your expectations? How so? And if not, how so?

I believe I had a great experience with other lab members, and it met all my initial expectations. Even though I have not completed everything I planned, I still gathered valuable data and still have time in the following semester.

- What did you not like about the experience? What surprised you about the research Experience?

I wished experiments took less time, because I needed to actively look for my samples for 32 hours for one experiment. I had seven of those experiments, and I could easily forget to take out the sample within those 32 hours or not check the temperature conditions.

- How did you connect with your faculty mentor and others with who you worked?

I had to submit a progress report and present my literature review slides every other week. I got to know my mentor and other members better through these small meetings and their feedback. We had a positive relationship and worked out issues very well.

- Would you recommend a summer research experience to your friends?

Yes, I think it introduces a new experience.

- Any advice for next summer's undergraduate research students?

Be patient and responsible when working on research, since it might take a while until you get any valuable results.

- Was your project an interdisciplinary project? From what backgrounds did your other

research colleagues come? What did you gain from this interdisciplinary project that you might not have experienced otherwise?

Our lab is very diverse and includes studies in biology, chemistry, physics, and engineering. I have been exposed to different projects, and I have worked on the chemical and engineering sides of the corrosion issue.

B. What are your future plans? Do you see yourself going into industry, graduate school professional school, etc. Did your summer experience impact your future plans?

I am not sure about specifics, but I am planning on applying to graduate school in the future.

C. Were the research education sessions helpful and/or informative? If so, which ones? What are Your thoughts regarding a day conference in June and/or July instead of the weekly sessions?

I think they were somewhat helpful, but they were not related to my field of study. The only session that I found really insightful was the Path to PI, because the presenter told a lot about their own academic career experience.

D. Please note whether you may have the opportunity to present your project as a poster or paper at a professional association conference. Will you co-author a journal article based on at least partially on your work?

I am not sure about co-authoring, but I think I can present at a conference when I get more results from my studies.

upon